Multidimensional shaping of ultrafast optical waveforms

Marc M. Wefers and Keith A. Nelson

Department of Chemistry, Massachusetts Institute of Technology, Cambridge, Massachusetts 02139

Andrew M. Weiner

School of Electrical Engineering, Purdue University, West Lafayette, Indiana 47907-1285

Received February 1, 1996

Simultaneous temporal and spatial shaping of ultrashort optical pulses is demonstrated. A two-dimensional mask pattern is used to filter spatially separated frequency components along one coordinate and to impart a shaped spatial (or wave-vector) profile along the perpendicular coordinate, yielding a spatially and temporally coherent output waveform. As an example, a single input pulse is transformed into 11 spatially separated output beams, each with an independently specified temporal profile. © 1996 Optical Society of America

Considerable attention has been given recently to the shaping of ultrashort optical pulses into waveforms with arbitrary temporal profiles.[1–8] Advances have included the use of programmable masks for computer-controlled waveform generation,[3–8] the shaping of sub-20-fs pulses,[7] and overall improvements in fidelity.[8] Applications of such waveforms to coherent control of quantum-mechanical systems have already been demonstrated, and further results can be anticipated.[9–12] The optical processing of shaped waveforms and their interconversion to and from spatial images by means of spectral holography have also been reported.[13–15] More recently, ultrafast time-varying two-dimensional spatial images have been generated by volume holographic techniques.[16]

In this Letter we demonstrate combined temporal and spatial shaping of ultrashort optical pulses based on linear spectral filtering of spatially separated frequency components. This permits generation of coherent high-fidelity ultrashort optical waveforms with tailored profiles along both the propagation direction, i.e., the temporal coordinate, and one perpendicular direction, i.e., one spatial coordinate. This is a logical extension of our earlier study of high-fidelity temporal pulse shaping[8] and profoundly expands the possible complexity of the waveforms produced. Temporal and spatial pulse shaping offers novel possibilities for manipulation of propagating excitations and other nonlocal material responses[17] and permits a large multiplex advantage in terahertz-bandwidth optical signal generation.

Temporal and spatial pulse shaping is made possible by use of both spatial dimensions of a mask placed in the focal plane of a zero-dispersion 4-f grating and lens apparatus, as shown in Fig. 1. This setup is identical to those described previously,[1,3,6,8] except that, following the first grating, which disperses the frequency components of the incident pulse along the horizontal or x axis, a cylindrical lens with curvature along the x axis rather than a spherical lens is used. With a spherical lens the spatially separated frequency components are focused to different regions of a horizontal line across the mask, and a horizontally oriented mask pattern is used for phase or amplitude filtering or both of selected frequency components. With a cylindrical lens each of the horizontally separated frequency components is spread out along the y axis, so a large two-dimensional area of the mask is irradiated. Many horizontally oriented mask patterns, separated in the vertical direction, can be used for temporal shaping of vertically separated strips of dispersed light. More generally, the mask patterns in the vertical direction are used for spatial (or wave-vector) shaping of the filtered light. As in earlier pulse shaping setups, a subsequent spherical lens and an antiparallel grating are used to recombine the spectrally filtered frequency components.

A second spherical lens, following the pulse shaping apparatus, is used to image the spatial pattern (along the y axis) imparted by the mask onto the sample while focusing the beam along the horizontal direction. The sample in this case is a KTP doubling crystal within which the shaped output and a variably delayed, unshaped pulse that is cylindrically focused to a vertical strip are overlapped spatially. The frequency-doubled light that arises when different spatial regions of the beams are time coincident provides a spatially varying cross-correlation pattern that is imaged onto a CCD camera, producing temporally resolved spatial images of the shaped waveform. An 80-fs, 10-μJ pulse at 788 nm from a 1-kHz titanium:sapphire regenerative amplifier was used to generate both the input pulse (8 μJ) and the unshaped reference pulse (2 μJ).

As a demonstration, we used a prefabricated phase mask consisting of ~28 separate horizontal patterns upon a 9 mm × 7 mm area of a fused-silica substrate. The patterns are designed to generate pulse sequences with slightly different terahertz-frequency repetition rates. Unlike previous experiments that used these masks,[12,18] the incoming beam is not focused along the y direction, so different horizontal strips of the spectrally dispersed light in the focal plane are incident onto many (~11) different patterns rather than onto a single pattern. Light between these strips is blocked by reflecting regions between the adjacent patterns on the mask. In this particular case it may seem appropriate to describe the procedure as multiplexed or parallel pulse shaping in which 1 beam enters and 11 beams,

0146-9592/96/100746-03$10.00/0

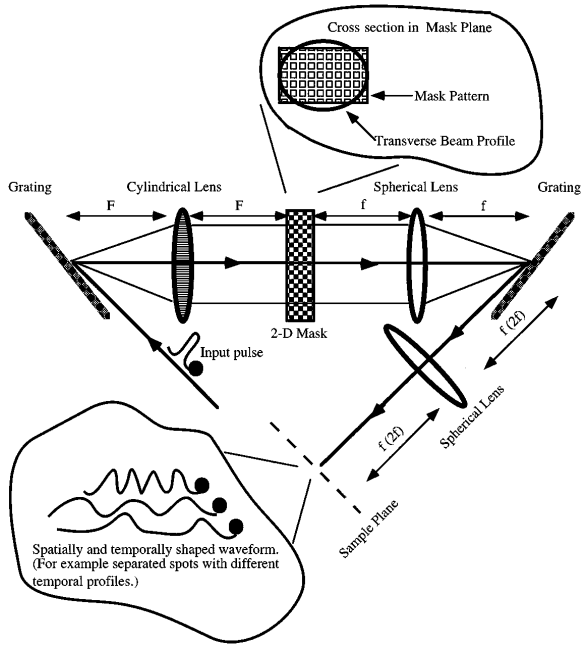

Fig. 1. Apparatus used for generation of multidimensional ultrafast optical waveforms. The pulse shaper consists of two antiparallel 1200-line/mm gratings at an incident angle of 45.25°, a 20-cm (focal length F) cylindrical lens (curvature along the x axis), two 15-cm (focal length f) spherical lenses, and a two-dimensional mask (2-D). The first grating disperses the frequency components of the incident pulse along the x (horizontal) axis. The cylindrical lens focuses the separated components onto different, horizontally separated regions of the mask but leaves them unfocused along the vertical (y-axis) direction. The mask filters different frequency components along the x axis and different spatial or wave-vector components along the y axis. The subsequent spherical lens and antiparallel grating recombine the spectrally filtered frequency components. A second 15-cm spherical lens is positioned to form a one-to-one telescope with the spherical lens following the mask, so the vertical spatial pattern of light immediately following the mask is imaged onto the sample. Characterization is performed by use of a doubling crystal as the sample and by cross correlation with a variably delayed unshaped reference pulse, which is focused to a vertical line and overlaps the shaped beam. To filter vertical wave-vector instead of spatial components, one could position the second spherical lens a distance $2f$ (rather than f) from both the sample and the second grating, thereby imaging onto the sample the spatial profile of the beam immediately after the grating.

each with an independently controlled temporal profile, emerge. However, it is important to realize that for an arbitrary two-dimensional mask (including the one used here) the shaped waveform is both temporally and spatially coherent.

Figure 2 shows cross-correlation images of the shaped waveform. At zero time delay (Fig. 2a), 11 separate 175-μm spots are visible. Ten of the spots consist of pulse trains with repetition rates ranging from 2.00 to 2.41 THz, all of which include a pulse at zero time delay. The second spot from the top consists of only a single pulse, which is time delayed but somewhat lengthened and of sufficient intensity to produce signal at zero time delay. At a 170-fs time delay (Fig. 2b), only the spot associated with the single pulse produces signal. At longer time delays (Figs. 2c–2e) the pulses in the different pulse trains are no longer temporally coincident as expected for pulse trains of varying repetition rates.

Figure 3 shows a cross-correlation measurement of each of the 11 separated spots in the shaped waveform, recorded separately with a 100-μm pinhole to isolate the frequency-doubled light from each spot. The central pulse is more intense than the other pulses in each of the pulse trains because the etch depth of the phase mask was optimized for 620-nm rather than the 788-nm wavelength used currently. The figure clearly shows well-defined pulse trains of varying repetition rates, as well as the single time-delayed pulse (second from the top). A dotted line is placed along time delay −1.37 ps (corresponding to Fig. 2d) to emphasize the varying repetition rates. The signal levels in the top and the bottom cross correlations are relatively weak because the shaped and reference beam intensities were relatively low near their top and bottom edges.

In this example the spatial image associated with the vertical dimension of the mask is directly imparted to the shaped waveform in the plane of the sample. Hence the spatial resolution of the shaped waveform is directly related to the spatial resolution of the mask. In some cases it will be desirable to produce shaped waveforms with finer spatial features. In such

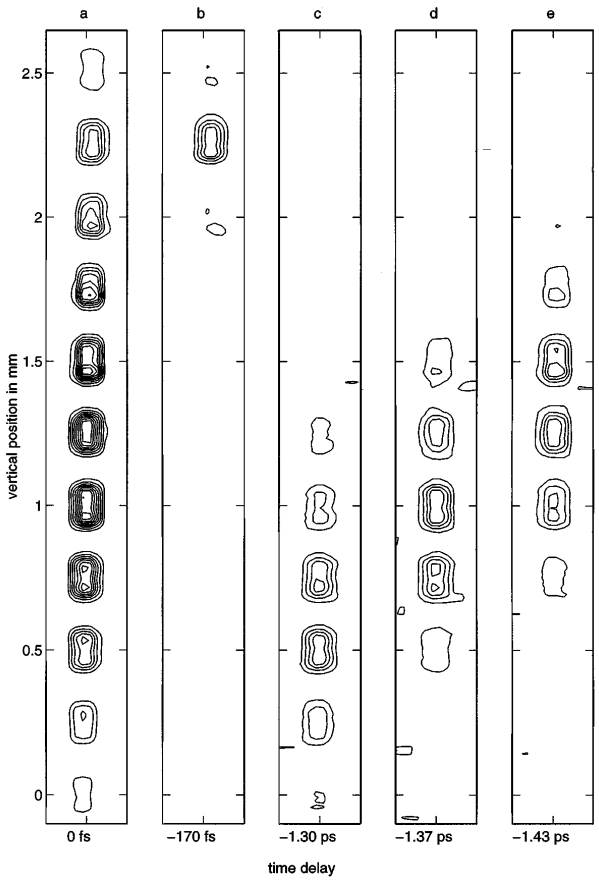

Fig. 2. Cross-correlation images of the shaped waveform at different times. The images show that different spots appear and disappear on femtosecond time scales.

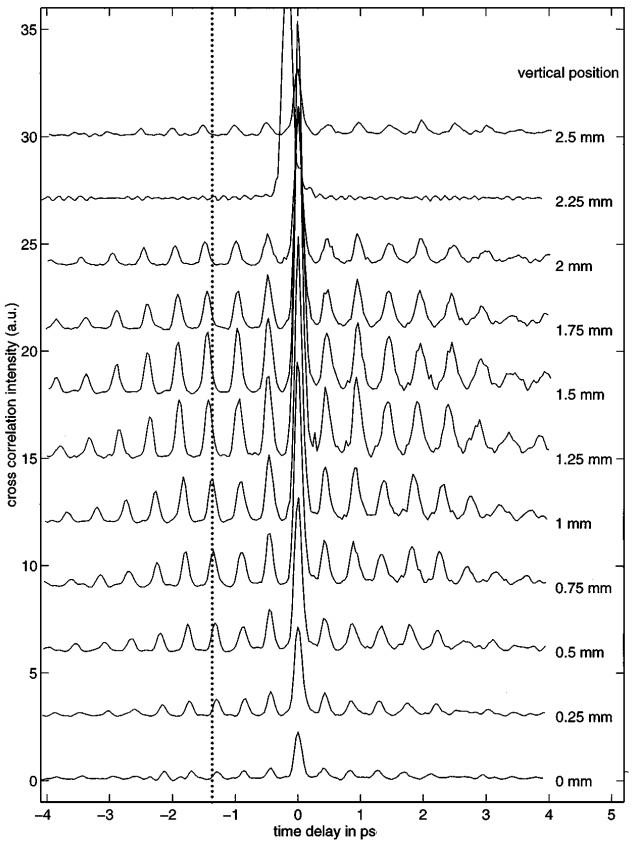

Fig. 3. Spatially resolved cross-correlation measurements of the shaped waveform. The waveform consists of 11 spots separated by 250 μm. The cross correlation of each spot shows a sequence of equally spaced femtosecond pulses. A dotted line is placed along time-delay -1.37 ps to illustrate the varying repetition rate between adjacent spots and to provide a comparison with Fig. 2d, which shows the spatial profile at this delay time.

cases it will be better to use the relatively large vertical aperture of the mask to filter vertical wave-vector (rather than the vertical spatial) components of the beam. Wave-vector filtering requires no change whatsoever in the pulse shaping setup but only a change in the subsequent imaging of the shaped waveform. Rather than imaging the vertical beam pattern immediately following the mask, one should image the shaped waveform immediately after the second grating to produce spatial features that can be diffraction limited (to $\sim$10-μm sizes with the current setup) along the vertical axis. Filtering of the vertical wave-vector components in the masking plane couples spatial and temporal shaping so that a particular horizontal frequency pattern is no longer uniquely related to a single spatial region of the output beam. Nonetheless an appropriate mask pattern can be determined easily from the two-dimensional Fourier transform of the time–space profile of the desired shaped waveform, normalized by the corresponding two-dimensional Fourier transform of the input waveform. This situation is entirely analogous to two-dimensional spatial Fourier filtering of wave fronts,[19] with the exception that the horizontal dimension of the mask is used to filter spatially separated frequency components rather than horizontal wave-vector components. We note that in general there is also a small degree of spatial shaping of the waveforms along the x axis that is due to diffraction effects that arise from imperfect spectral resolution along this axis.[20,21]

In conclusion, we have demonstrated coherent spatial and temporal shaping of ultrafast optical waveforms. The present results, achieved with a permanent phase mask, should motivate the development of programmable two-dimensional masks for more-complex and versatile multidimensional ultrafast optical waveform generation.

This research was supported in part by National Science Foundation grant CHE-9404548.

References

1. A. M. Weiner, J. P. Heritage, and E. M. Kirschner, J. Opt. Soc. Am. B **5,** 1563 (1988).
2. D. Brady, A. G. S. Chen, and G. Rodriguez, Opt. Lett. **17,** 610 (1992).
3. A. M. Weiner, D. E. Leaird, J. S. Patel, and J. R. Wullert, IEEE J. Quantum. Electron. **28,** 908 (1992).
4. M. Haner and W. S. Warren, Appl. Phys. Lett. **52,** 1458 (1988).
5. C. W. Hillegas, J. X. Tull, D. Goswami, D. Strickland, and W. S. Warren, Opt. Lett. **19,** 737 (1994).
6. M. M. Wefers and K. A. Nelson, Opt. Lett. **18,** 2032 (1993).
7. A. Efimov, C. Schaffer, and D. H. Reitze, J. Opt. Soc. Am. B **12,** 1968 (1995).
8. M. M. Wefers and K. A. Nelson, Opt. Lett. **20,** 1047 (1995).
9. W. S. Warren, H. Rabitz, and M. Dahleh, Science **259,** 1581 (1993).
10. H. Kawashima, M. M. Wefers, and K. A. Nelson, Ann. Rev. Phys. Chem. **46,** 627 (1995).
11. I. Brener, P. C. M. Planken, M. C. Nuss, L. Pfeifferm, D. E. Leaird, and A. M. Weiner, Appl. Phys. Lett. **63,** 2213 (1993).
12. A. M. Weiner, D. E. Leaird, G. P. Wiederrecht, and K. A. Nelson, Science **247,** 1317 (1990).
13. A. M. Weiner, D. E. Leaird, D. H. Reitze, and E. G. Paek, Opt. Lett. **17,** 224 (1992).
14. M. C. Nuss, M. Li, T. H. Chiu, A. M. Weiner, and A. Partovi, Opt. Lett. **19,** 664 (1994).
15. M. C. Nuss and R. L. Morrison, Opt. Lett. **20,** 740 (1995).
16. K. B. Hill, K. G. P. Purchase, and D. J. Brady, Opt. Lett. **20,** 1201 (1995).
17. K. A. Nelson, "Coherent control: optics, molecules, and materials," in *Ultrafast Phemonena IX*, G. A. Mourou, A. H. Zewail, P. F. Barbara, and W. H. Knox, eds. (Springer-Verlag, Berlin, 1994), pp. 47–49.
18. A. M. Weiner and D. E. Leaird, Opt. Lett. **15,** 51 (1990).
19. G. R. Fowles, *Introduction to Modern Optics* (Holt, Rinehart &Winston, New York, 1968) pp. 133–144.
20. M. M. Wefers and K. A. Nelson, J. Opt. Soc. Am. B **12,** 1343 (1995).
21. M. M. Wefers and K. A. Nelson, IEEE J. Quantum Electron. **32,** 161 (1996).